Desalination and Water Treatment 318 (2024) 100313

Contents lists available at ScienceDirect

Desalination and Water Treatment

journal homepage: www.sciencedirect.com/journal/desalination-and-water-treatment/

Performance of hydrogel beads composites derived from sodium alginate-cetyltrimethylammonium bromide toward congo red dye adsorption from aqueous solution

Endar Hidayat[a,b,c,*], Nur Maisarah Mohamad Sarbani[a,b], Helmi Baharuddin Susanto[b,d], Yaressa Vaskah Situngkir[b,e], Marchanda Wahyu Chrisandi[b,e], Sadaki Samitsu[c], Yoshiharu Mitoma[f], Seiichiro Yonemura[a,b], Hiroyuki Harada[a,b]

[a] Graduate School of Comprehensive Scientific Research, Prefectural University of Hiroshima, Shobara 727-0023, Japan
[b] Department of Life Systems Science, Faculty of Bioresources Science, Prefectural University of Hiroshima, Shobara 727-0023, Japan
[c] Data-driven Polymer Design Group, Research Center for Macromolecules and Biomaterials, National Institute for Materials Science, 1–2-1 Sengen, Tsukuba 305-0047, Japan
[d] Department of Renewable Energy Engineering, Politeknik Negeri Jember, Jember 68121, Indonesia
[e] Department of Agricultural Engineering, Politeknik Negeri Jember, Jember 68121, Indonesia
[f] Department of Integrated Science and Engineering for Sustainable Societies, Faculty of Science and Engineering, Chuo University, Tokyo 112-8551, Japan

ARTICLE INFO

Keywords:
Hydrogel bead
Sodium alginate
Cetyltrimethylammonium bromide
Congo red dye adsorption
Wastewater treatment

ABSTRACT

The complex process for treating industrial wastewater frequently necessitates the employment of efficient treatment techniques to eliminate harmful contaminants before discharge, such as congo red (CR) dye. In this study, adsorption methods were utilized to eliminate CR by employing hydrogel bead composites derived from sodium alginate (SA) and cetyltrimethylammonium bromide (CTAB). Various concentrations of CTAB, including 0.1 wt%, 1 wt%, and 3 wt%, denoted as SC1, SC2, and SC3 respectively, were examined. The results demonstrated that SC3 has higher swelling percentage and lowest carboxyl group (COOH). Experiments were carried out under different pH levels, CR concentrations, and adsorption durations for removal of CR. The maximum CR adsorption capabilities of SC1, SC2, and SC3 obtained were as 141.08 mg/g, 144.50 mg/g and 153.24 mg/g for SC1, SC2 and SC3, respectively. The Freundlich and pseudo-second-order models demonstrate the best fit for both isotherm and kinetic analysis across all samples, suggesting a multilayer adsorption process and chemisorption mechanism. Reusability studies revealed strong performance, underscoring the hydrogel beads' potent adsorption capability for CR dye.

1. Introduction

Dyes find extensive application in the textile and printing sector [1,2]. The majority of these dyes consist of organic compounds, characterized by their toxicity, stability, and resistance to environmental degradation [3]. Despite undergoing primary treatment, large-scale release of dye containing materials from industrial effluent like textile mills and printing company could pose a significant threat to aquatic ecosystems. The constituents commonly utilized in the dyeing industry encompass various organic substances, predominantly reactive dyes, disperse dyes, vat dyes, and direct dyes [4].

In 1884, Congo Red (CR) was discovered to have valuable functions as dye due to its great colouring qualities, simplicity and affordability which represented a significant achievement in the development of direct dyes [4]. Typically, direct dyes are predominantly of the azo type (comprising mono-azo and poly-azo compounds). Majority of synthetic dyes available nowadays are azo based, primarily derived from aniline compounds [5]. Hazardous pollutants like aniline compounds may pose severe environmental pollution and health risks. Since this notable direct dye of CR can exhibits carcinogenic properties and endanger the health of both human and animal; hence, removal of CR from effluents remains a critical concern [6].

Advanced physicochemical techniques such as ozonation [7], coagulation [8], membrane [9], electrocoagulation [10], chemical oxidation [11], biological [12], and etc, have been employed to remove CR dye. Nonetheless, these techniques are typically more costly and

* Corresponding author at: Graduate School of Comprehensive Scientific Research, Prefectural University of Hiroshima, Shobara 727-0023, Japan.
E-mail address: hidayatendar1@gmail.com (E. Hidayat).

https://doi.org/10.1016/j.dwt.2024.100313
Received 2 April 2024; Received in revised form 22 April 2024; Accepted 22 April 2024

inefficient, need a regulated environment and significant amounts of chemicals, as well as produce hazardous by-products that can lead to waste management issues [13]. For example, generating ozone requires significant energy input, often through ultraviolet (UV) light methods. The ion exchange approach is not appropriate for many types of dyes, whereas the membrane separation method typically generates sludge in a large amount. Additionally, only certain dyes can be mineralized by chemical oxidation, and this method is only practical economically to remove high concentration of dyes. The primary disadvantages of biological treatment are the necessity for exact pH condition and temperature control, slow response rate, and disposal of sludge [14]. Given these limitations, the adsorption process for removing CR dye appears to be the ideal option because of its relatively low operating expenses, excellent removal efficiency, ease of use, and reusable adsorbent [15].

Adsorbents such as banana peel powder [16], Citrus limetta peel powder [17], hydrochar [18], ZnO nanomaterial [19], FexCo3-xO4 [4], and $Fe(OH)_3$ @cellulose fibbers [20] have been frequently utilized for the adsorption of CR. However, their preparation takes a long time and involves complicated purifying procedures [21]. Alternatively, hydrogel beads are polymeric materials that are easily prepared, affordable, reusable, highly cross-linked, porous, and mechanically stable without the need for further purifying processes.

Hydrogel beads are three-dimensional, crosslinked polymer networks capable of absorbing and retaining large volumes of water or aqueous solutions [22]. Their tuneable properties, such as porosity, swelling behaviour, and surface chemistry, make them highly suitable for various applications, including water purification [23]. By integrating specific functional groups or additives, hydrogel beads can be tailored to selectively adsorb target pollutants, such as CR dye. Among the materials used in hydrogel bead synthesis, sodium alginate (SA) derived from brown algae, stands out as a biocompatible, renewable, and economically viable option [24–26]. Calcium (Ca) cations are frequently employed in crosslinking SA, leading to ion exchange and the formation of Ca alginate (CA) hydrogel. Furthermore, its molecular structure contains numerous hydroxyl (-OH) and carboxyl (-COOH) groups, making it an environmentally friendly choice for variety of dye molecules [27,28]. Numerous studies have explored the adsorption of CR dye by SA; nevertheless, the key improvement highlighted by many studies is mostly connected to the weak stability of SA. SA may be generated into stable configuration of hydrogel beads through the cross-linking with synthetic polymer material [29]. Various chemical modification techniques, such as cross-linking and the introduction of new functional groups, have been employed to improve stability and enhance SA's adsorption capacity [30,31].

Recently, surfactant-modified adsorbents, including biochar [32], iron oxide [33], and nanomaterial [34], have been utilized. Consequently, surfactant modification of SA for CR dye adsorption has been explored. Surfactants, characterized by their amphiphilic nature with hydrophilic and lipophilic components, are known to alter energy relationships at interfaces, typically by affecting surface or interfacial tension [35–37]. Hence, surfactants have been widely employed in modifying various adsorbents [38]. For instances, sodium dodecyl sulfate (SDS) [39–41], Poly (sodium styrene sulfonate) (PSS) [42], sodium lauryl [43], and cetyltrimethylammonium ammonium bromide (CTAB) [44]. These surfactants serve as stabilizers for adsorbents, acting as surface modifiers and exhibiting an affinity for surface reactions [45]. However, CTAB stands out as the best choice for this study owing to its stability in both alkaline and acidic conditions, robust surface activity, antibacterial characteristics, and cationic nature [46], facilitating the effective capture of CR dye through electrostatic attraction. Several reports have used CTAB as a surface modification of adsorbent and to enhance adsorption capacity of dyes such as activated biochar [47], chitosan-gelatin-CTAB composite [48], and organo-bentonite-CTAB [49]. However, to the best of authors` knowledge, the incorporation of CTAB with SA for CR dye adsorption has not been properly documented. Therefore, it was essential to assess their performance.

In this present study, we would like to evaluate the feasibility of using SA-CTAB hydrogel bead composite with different CTAB ratio as an effective adsorbent to remove CR. It is expected that this research could address the lack of comprehensive studies on the properties, characterization, and application of SA-CTAB composite for CR dye adsorption. The effects of several factors including pH, initial CR concentration, and duration were examined. Isotherm and kinetic models were employed to comprehend the adsorption mechanisms. Additionally, regeneration of CR adsorption was also examined.

2. Material and Method

2.1. Materials

Congo red dye (CR), calcium chloride ($CaCl_2$), hydrochloric acid (HCl) and sodium hydroxide (NaOH) were supplied from Kanto Chemical Co. Inc., Japan. Sodium alginate (SA) and Cetyltrimethylammonium bromide (CTAB) were purchased from Wako Chemical Industries, Osaka, Japan.

2.2. Hydrogel bead preparation

Preparation of hydrogel beads was done by mixing 20 mL of 1 wt% SA solution and 2 mL of CTAB aqueous solution with difference concentration: 0.1 wt%, 1 wt% and 3 wt%, referred as SC1, SC2 and SC3, respectively. After the solution was put into bottle flasks, it was shaken for 30 min at ambient temperature using a rotary shaker (Rotator RT-50). The solution was then gradually injected into 4 wt% $CaCl_2$ aqueous solution by using a 10 mL syringe. Next, the sample was allowed to cure for a full night in order to produce hydrogel beads. Afterward, the beads were allowed to dry in an oven for 24 h at 60 °C after being cleaned with ethanol and deionized water (DI).

2.3. Adsorption experiments

A series of experiments were executed to examine the impacts of several factors, such as initial pH, CR concentration, and adsorption duration, on the elimination of CR. Batch adsorption trials were performed by submerging the hydrogel bead sample in 50 mL of CR solution. The remaining concentration of CR after the experiment was analyzed using a UV-Vis spectrophotometer (JASCO V-530) at a wavelength of 562 nm. The formulas utilized for computing the removal percentage (Removal, %) (Eq. 1) and adsorption equilibrium quantity (q_e, mg/g) (Eq. 2) are outlined below.

$$\text{Removal } (\%) = \frac{C_i - C_e}{C_i} \times 100 \tag{1}$$

$$q_e = \frac{C_i - C_e}{W} \times V \tag{2}$$

where *Removal* % represents the efficiency of removal, with C_i and C_e denoting the initial and equilibrium concentrations of CR (mg/L), respectively. q_e stands for the adsorption capacity at equilibrium of the adsorbent (mg/g), while W signifies the quantity of adsorbent (g), and V indicates the volume of the CR solution (L).

2.4. Determination of carboxyl groups

A technique of conductometric titration was utilized to quantify the carboxyl (COOH) group of the hydrogel beads [50]. To achieve homogenous distribution, the dried hydrogel bead was incorporated with 2.5 mL of 20 mM NaCl solution for 30 min. Then, HCl was added into the mixture until the pH to achieve pH 3.0. Afterward, the mixture solution then incrementally adjusted to pH of 11.0 using a NaOH solution. The content of COOH group inside the hydrogel beads was assessed using the following Eq. (3).

$$\text{Carboxyl group content,COOH(mmol/g)} = \frac{V_{NaOH} \times M_{NaOH}}{W_d} \tag{3}$$

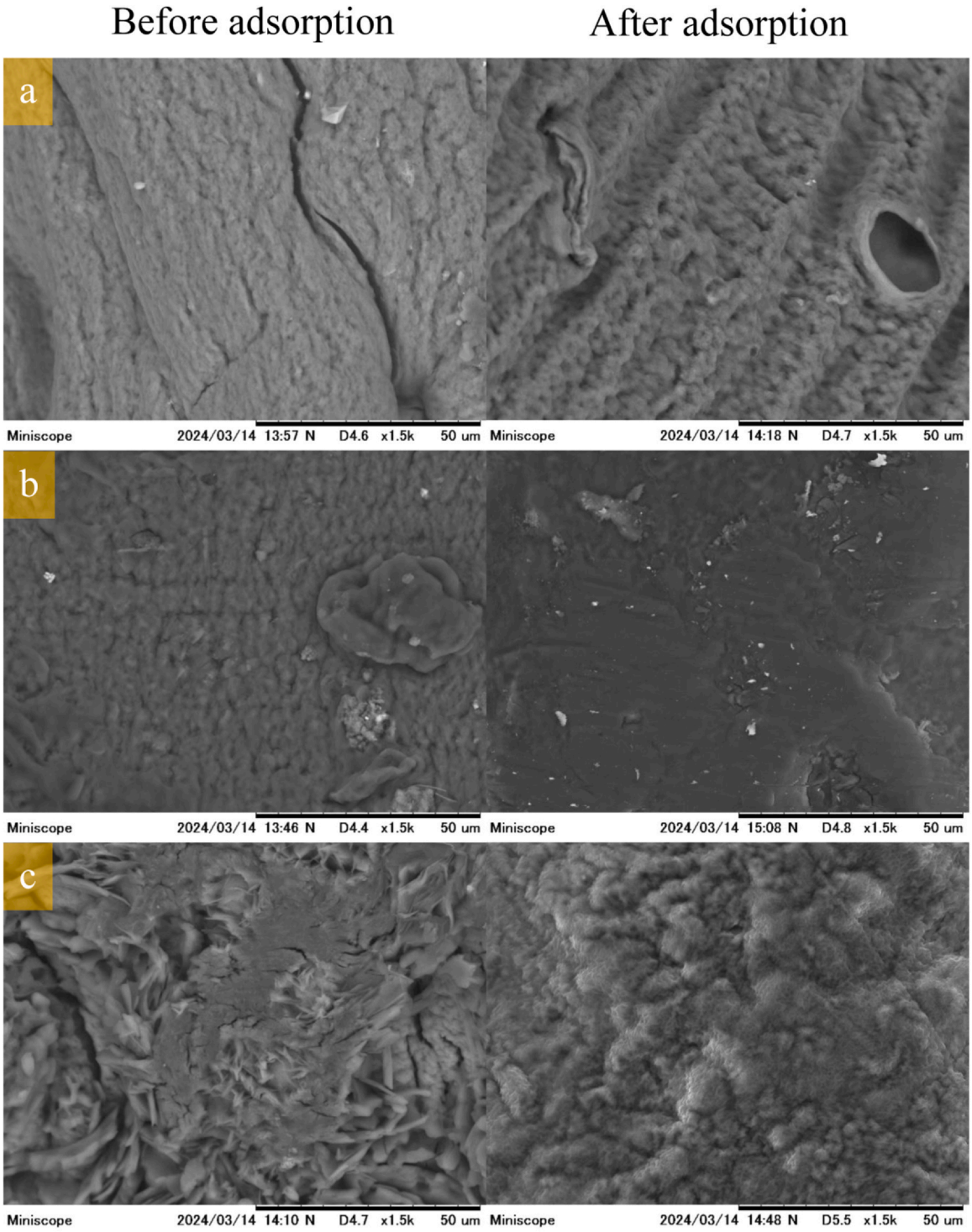

Fig. 1. SEM morphology of hydrogel beads (a) SC1 (b) SC2 (c) SC3.

where V_{NaOH} (mL) is the NaOH volume needed to deprotonate COOH groups. M_{NaOH} (mol/L) is the concentration of NaOH, while W_d (g) represents the initial weight of dry hydrogel beads.

2.5. Swelling properties

The swelling properties of the hydrogel composites were assessed using DI by performing the experiment using batch shaker for 24 h at room temperature. The percentage of swelling was estimated by applying the Eq. (4).

$$\text{Swelling } (\%) = \frac{W_s - W_d}{W_d} \times 100 \quad (4)$$

where W_s and W_d represent the weights of swollen hydrogel beads and dried hydrogel beads, respectively.

2.6. Analytical measurements

FTIR spectra were acquired utilizing a Thermo Scientific Nicolet iS10 instrument (Thermo Fisher Scientific Inc., Waltham, MA, USA) both prior to and after CR adsorption. The morphology of SA/CTAB

Table 1
Characteristics of hydrogel bead.

Sample	Swelling (%)	COOH (mmol/g)
SC1	49.67 ± 5.84	0.40 ± 0.06
SC2	96.50 ± 0.98	0.38 ± 0.03
SC3	162.28 ± 8.92	0.28 ± 0.06

based hydrogel beads were observed via scanning electron microscopy (SEM) (Miniscope TM3000, Hitachi-hitech, Tokyo, Japan). The pH_{zpc} value, indicative of the neutral surface charge was determined. Dried hydrogel beads were immersed with 10 mM NaCl with different pH between 2 and 8, then mixed for 24 h under room temperature. The pH_{zpc} calculated using the equation: ΔpH = pH-final − pH-initial [51].

3. Results and discussion

The morphology of hydrogel beads before and after CR adsorption acquired using Scanning electron microscopy (SEM) is presented in Fig. 1. According to Fig. 1, all samples exhibit a rough and wrinkle surface before adsorption experiment. The SC3 sample which contains the highest percentage of CTAB (3 wt%) has a rougher surface with multiple crystal-like shapes on its surface. After CR adsorption process, all of the samples showed changes on their morphology by becoming slightly smooth. It can be observed that there is a pore present on the surface of SC1 sample after adsorption.

Table 1 depicts the swelling percentage and the carboxyl groups content present in the hydrogel beads. The swelling percentage data demonstrate that higher CTAB concentration led to increase in swelling percentage. This is probably due to CTAB molecules that are amphiphilic, meaning they have both hydrophilic and hydrophobic parts. When CTAB concentration is high, the hydrophilic parts of the molecules may interact more strongly with the polymer chains, making the hydrogel beads more hydrophilic overall. This increased hydrophilicity can increase the affinity of the hydrogel towards water, thereby increasing swelling percentage.

Likewise, increase CTAB concentrations may lead to a decline in the COOH content of the hydrogel bead composite. This could be attributed to the competitive binding of CTAB, which competes for available binding sites on the alginate polymer chains. As CTAB molecules bind to these chains, they may occupy sites that would otherwise be utilized by Ca ions for cross-linking the alginate molecules. This competition for binding sites ultimately reduces the overall cross-linking density of the hydrogel beads, subsequently decreasing the COOH content.

The FTIR spectra of the hydrogel bead before and after CR adsorption are depicted in Fig. 2. The peak in the range of 3200 cm^{-1} to 3500 cm^{-1} corresponds to OH groups [52]. A new peak emerged after CR adsorption in the range of 2849 cm^{-1} to 2920 cm^{-1}, attributed to methylene group [17]. Another peak at approximately 1590 cm^{-1}, assigned to the stretching of $–COO^-$ [53,54], and a peak at around 1023 cm^{-1} representing the C-O stretching vibrations [28]. IR analysis suggest that intermolecular forces involving the functional components of hydrogel beads and CR dye molecules likely contribute to dye adsorption, alongside with electrostatic attraction. Possible mechanisms of CR dye adsorption onto hydrogel bead composite as shown in Fig. 3.

3.1. Initial pH effect analysis

The pH level of solution influences both the charged state of the CR and the charge surface of the hydrogel bead [55]. Fig. 4a illustrates the adsorption behaviour of CR as the pH of the CR solution varies. The

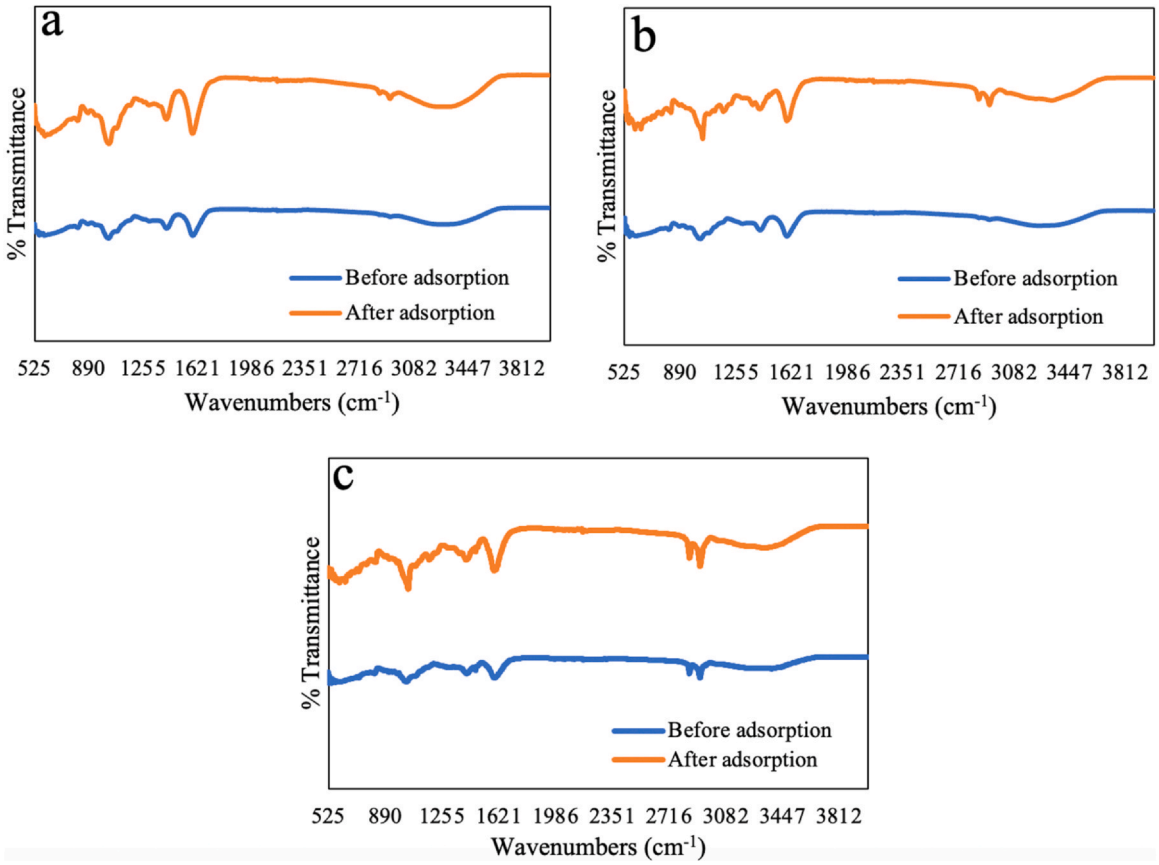

Fig. 2. FTIR spectra of hydrogel bead before and after CR adsorption. (a) SC1 (b) SC2 (c) SC3.

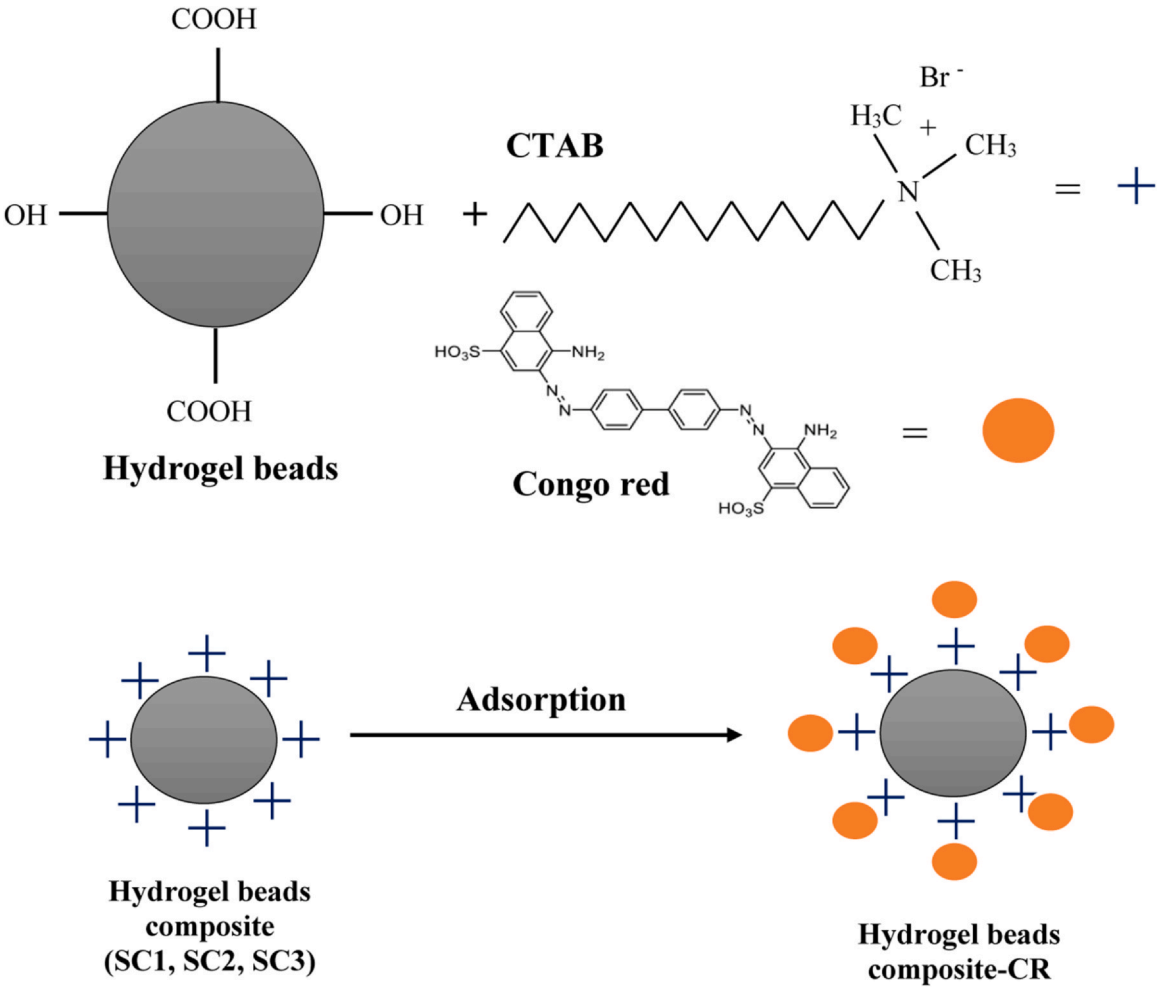

Fig. 3. Proposed mechanisms of CR adsorption.

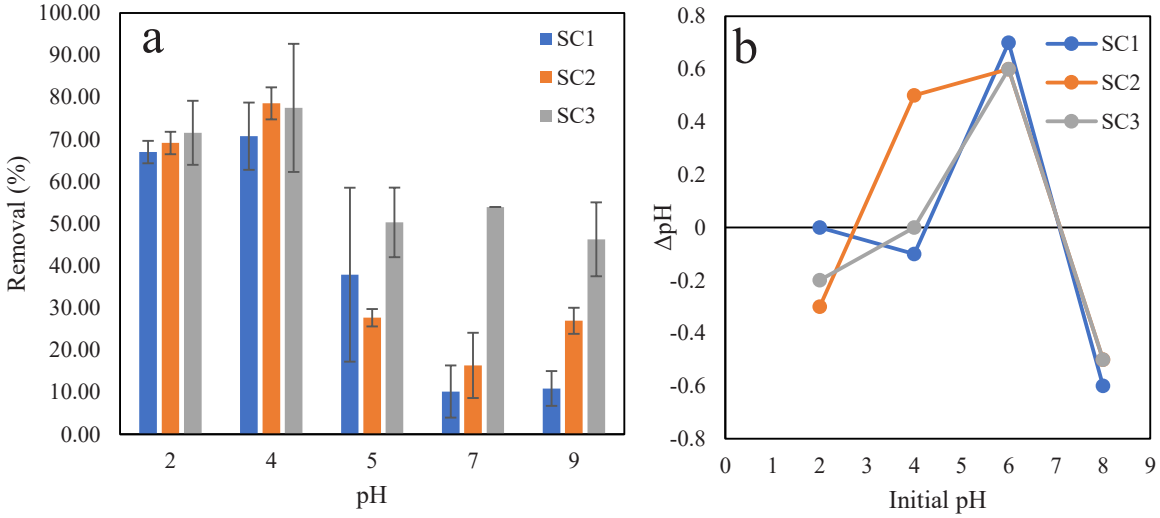

Fig. 4. (a) Effect of pH versus removal percentage (b) surface charge of hydrogel beads.

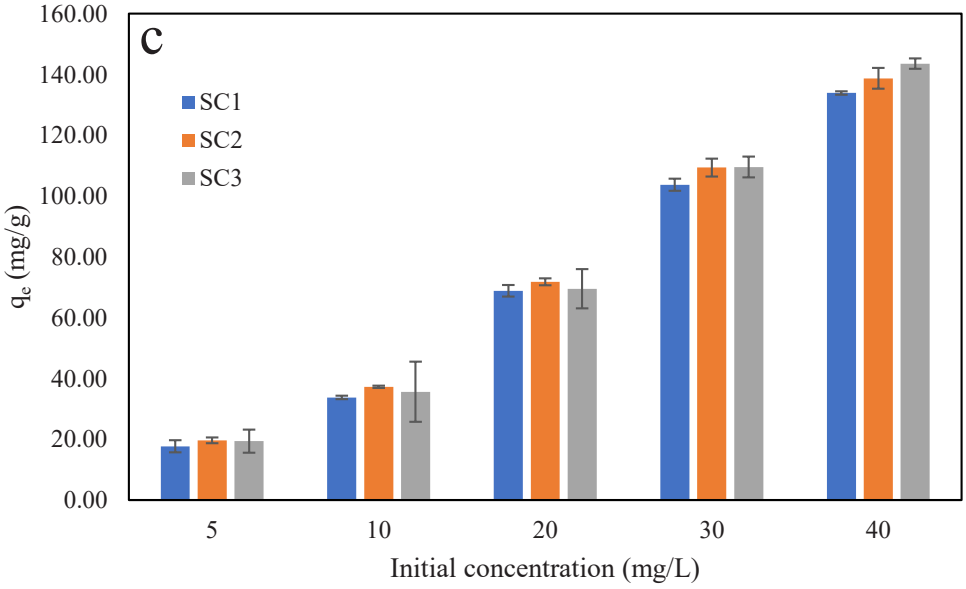

Fig. 5. Effect of initial CR concentration versus adsorption capacity. Initial pH 4 for SC1, SC2 and SC3.

Table 2
Isotherm model parameters for adsorption CR dye.

Isotherm models	Parameters	Samples		
		SC1	SC2	SC3
Langmuir	R^2	0.3645	0.8217	0.2124
Freundlich		0.996	0.9956	0.9815
Freundlich	K_f (g/mg $min^{-1})^n$	301.0243	778.2555	583.2367
	1/n	0.9479	0.8231	0.8820

removal percentage initially increases, and then decreases within the pH range of 2 to 9. The graph shows that pH 2 provides optimal condition for SC1, SC2 and SC3, resulting in an optimum removal percentage of 70.75%, 78.55% and 77.47%, respectively. Fig. 4b show the surface charges of the hydrogel bead. The data revealed that the samples, namely, SC1, SC2 and SC3 exhibited negative charges below pH_{zpc} values of 4.2, 2.6 and 4.0, respectively, while CR dye exhibits a positive charge under acidic conditions due to protonation. This observation indicates that the electrostatic attraction between the hydrogel beads and CR dye. A comparable outcomes of CR adsorption onto CTAB modified pumice [56] and tea waste [57] have been reported.

3.2. Initial concentration effect analysis

The adsorption of CR onto hydrogel beads was examined by adjusting the initial CR concentration in the range of 5 to 40 mg/L. This experiment was conducted for 30 min, at pH 4 for SC1, SC2 and SC3, respectively, and an adsorbent dosage of 10 mg/50 mL. The results demonstrated that increasing the CR concentration to 40 mg/L resulted in enhanced CR adsorption capacity in the hydrogel beads for all samples (Fig. 5). As the initial CR concentration increases, a greater concentration gradient is established between the CR solution and the hydrogel bead surface. This amplifies the driving force for adsorption, thereby attracting and capturing more CR dye molecules onto the hydrogel bead material.

3.3. Adsorption isotherm analysis

The adsorption isotherm helps to clarify the relation between the adsorbent hydrogel bead and CR dye, thereby enhancing our comprehension of the adsorption process. In this study, we utilized Langmuir (Eq. 5) and Freundlich (Eq. 6) models to evaluate the data derived from the adsorption experiments. Table 2 presents the linear regression coefficient (R^2) values obtained from Fig. 6, along with additional characteristics of the adsorption isotherms. The result observed show that Freundlich model suit the adsorption data compared to the Langmuir model across all samples, as indicated by the higher R^2 values. The 1/n values showed indicate a favourable adsorption process as the value being less than 1. These results suggest that a multilayer-like adsorption occurred at the adsorption sites of hydrogel beads.

$$C_e/q_e = \left(\frac{C_e}{q_{max}}\right) + 1/(K_L q_{max}) \tag{5}$$

$$\ln q_e = \ln K_F + \frac{1}{n} \ln C_e \tag{6}$$

In this context, q_e (mg/g) represents the adsorption capacity, C_e (mg/L) denotes the equilibrium concentration, q_{max} (mg/g) signifies the maximum adsorption capacity, R_L indicates a coefficient reflecting the stronger of adsorption, K_L (L/mg) and K_F (mg/g) represent the equilibrium constants of adsorption, and *1/n* signifies the adsorption intensity.

3.4. Adsorption kinetic analysis

An adsorption kinetic model serves as a mathematical framework employed to depict the pace of adsorption progression as time elapses. These models are designed to elucidate the underlying mechanisms and dynamics of adsorption phenomena by quantifying alterations in the concentration of the adsorbate (CR dye) within the adsorbent (hydrogel bead) over time. The impact of varying adsorption durations (30–1440 min) on the adsorption of CR using hydrogel bead at a concentration of 40 mg/L is shown in Fig. 7. The observations indicate that the adsorption of CR fluctuated over a period of 1440 min for all hydrogel bead samples. This evidenced that a higher concentration of CTAB in the hydrogel beads resulted in an increased adsorption capacity for the CR dye. This suggests that the swelling rate and COOH group content (Table 1) affect the adsorption of CR dye. Ultimately, equilibrium was reached after 1440 min, with adsorption capacity of 141.08 mg/g, 144.50 mg/g, and 153.24 mg/g for SC1, SC2, and SC3, respectively.

The kinetic data provided significant insights on the adsorption process. The data collected from the CR adsorption on the hydrogels

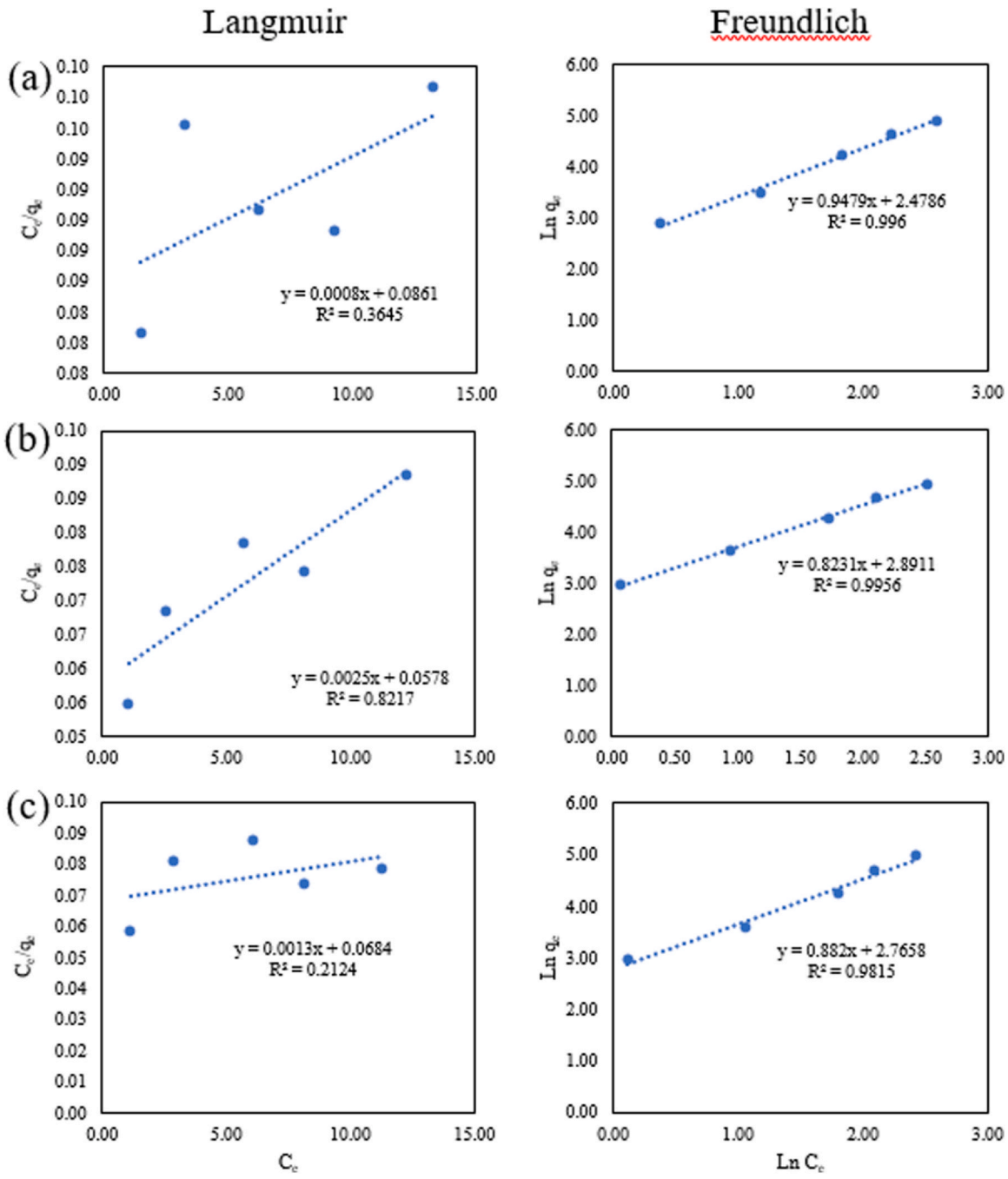

Fig. 6. Isotherm model of CR adsorption (a) SC1 (b) SC2 (c) SC3.

were examined using kinetic models: the first-order in Eq. (7) and second order models in Eq. (8).

$$\log(q_e - q_t) = \log q_e - K_1 t \quad (7)$$

$$t/q_t = 1/(K_2 q_e^2) + t/q_e \quad (8)$$

where K_1 (min^{-1}) is the rate constant of the pseudo-first-order model and t (min) is the time. K_2 is the constant rate of pseudo-second-order models.

Fig. 8 and Table 3 show the linear correlation coefficients and kinetic variables for CR adsorption. The first-order kinetic model obtained a significantly lower R^2 value than the second-order kinetic model for all hydrogel bead samples. Thus, the adsorption process is regulated by chemisorption. The finding was corresponded with previous studies conducted by [58,59] who used CS/ZL/ZrO/Fe_3O_4 and chitosan polyacrylamide hydrogels for phosphate and CR adsorption, respectively.

3.5. Regeneration of CR dye adsorption

Studying the regeneration of CR dye adsorption is crucial for comprehending the adsorbent's efficacy in capturing CR molecules repeatedly. In the analysis of hydrogel bead regeneration, a combination of acetone and DI water was employed to cleanse the CR dye from the adsorbent surface. Fig. 9 illustrates the reusability of this hydrogel for up to three cycles. The findings indicate that SC1 exhibited fluctuating trends of increase and decrease, whereas SC2 displayed a consistent decrease. Conversely, SC3 demonstrated a stable performance in adsorption capacity. From this, it can be inferred that the concentration of CTAB has an impact on CR dye adsorption.

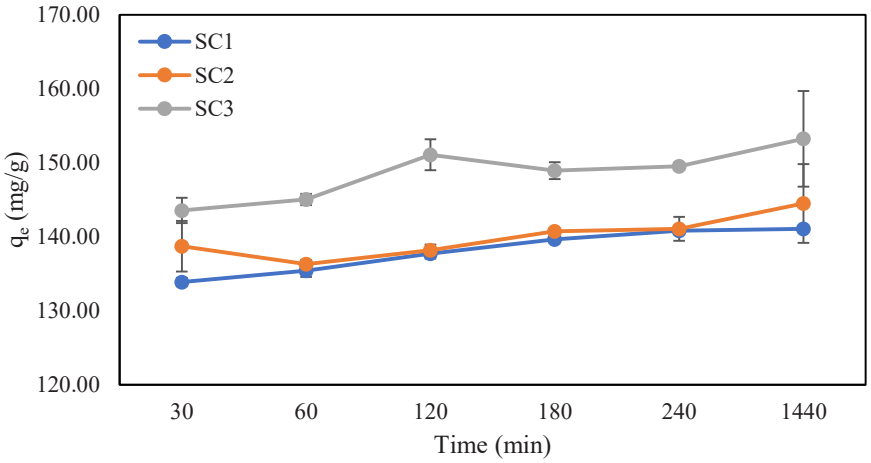

Fig. 7. Effect of contact time versus adsorption capacity. Initial pH: 4, Initial CR concentration: 40 mg/L.

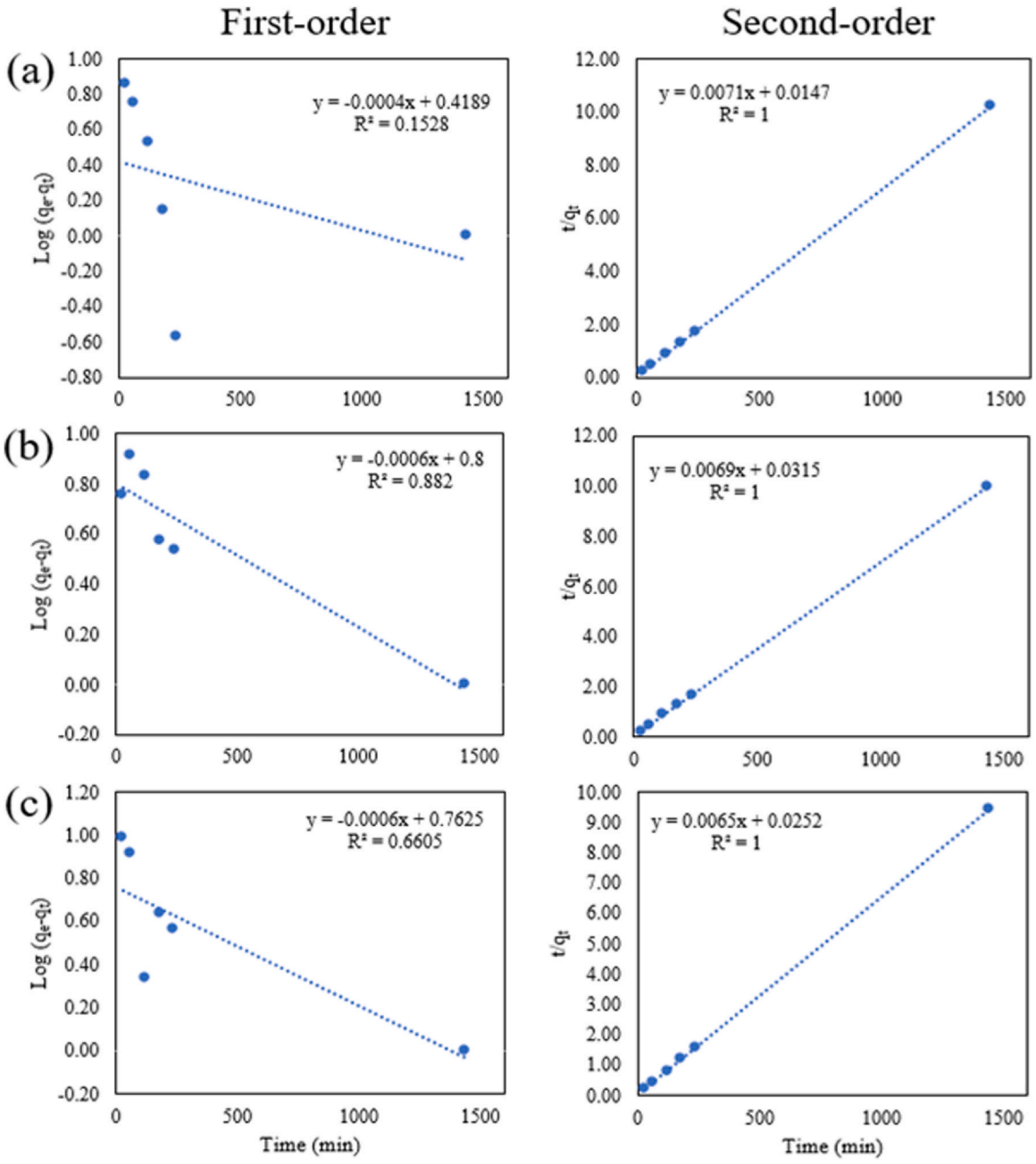

Fig. 8. Kinetic model of CR adsorption. (a) SC1 (b) SC2 (c) SC3.

Table 3
Kinetic model parameters for adsorption CR dye.

Kinetic models	Parameters	Samples		
		SC1	SC2	SC3
First-order	R^2	0.1528	0.882	0.6605
Second-order		1	1	1
Second-order	q_e (mg/g)	140.8451	144.9275	153.8462
	K_2 (g/mg min^{-1})	0.0034	0.0015	0.0016

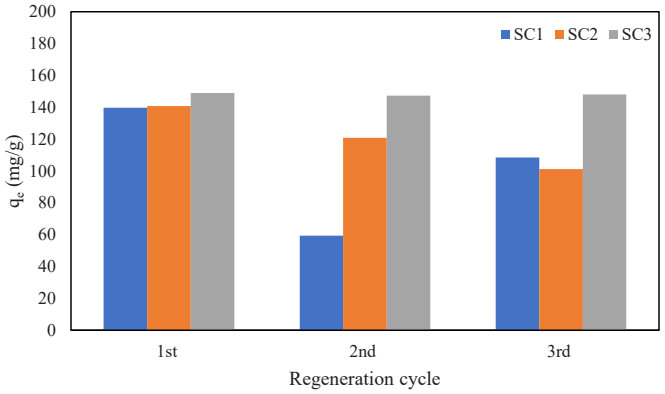

Fig. 9. Regeneration of CR dye adsorption.

Table 4
Comparison adsorbents for CR adsorption.

Adsorbent	q_e (mg/g)	Reference
Fly ash	22.12	[60]
$ZnCr_2O_4$ oxide	44.03	[61]
$MgCr_2O_4$ oxide	43.59	[61]
$CoCr_2O_4$	28.71	[61]
2Clph-BU-Cs	93.46	[62]
CS-DE@CA	23.28	[63]
DE@CA	38.84	[63]
Na_2SiO_3-CTAB	73.04	[64]
SC1	141.08	This study
SC2	144.50	This study
SC3	153.24	This study

3.6. Comparison between SC1, SC2, SC3 and other adsorbents to remove CR dye

To evaluate the efficacy of this adsorbent, it is notable to compare the adsorption capacity (Q) of the SC1, SC2, and SC3 adsorbents towards the anionic CR dye, with those of previously published adsorbents, as shown in Table 4. Of all the adsorbents reported in the literature, it can be certainly differentiated that SC1, SC2, and SC3 show the greatest qe for CR dye adsorption.

4. Conclusion

This research uncovered the remarkable effectiveness of the hydrogel beads composite in removing CR from aqueous solutions. Factors influencing the sorption process of CR dye included CTAB concentrations (0.1 wt%, 1 wt%, and 3 wt%, referred to as SC1, SC2, and SC3, respectively), pH levels, initial CR concentration, and duration. The results demonstrated that increasing CTAB concentration led to increased swelling percentage and decreased carboxyl group. Impressively, the adsorption capacity for CR were measured at 141.08 mg/g, 144.50 mg/g and 153.24 mg/g for SC1, SC2 and SC3, respectively. Isotherm and kinetic models were fitted Freundlich and pseudo-second-order models. These results strongly suggest a complex adsorption mechanism characterized by multilayer formations and chemical interactions.

CRediT authorship contribution statement

Marchanda Wahyu Chrisandi: Formal analysis, Data curation. **Sadaki Samitsu:** Validation, Methodology. **Yoshiharu Mitoma:** Data curation. **seiichiro Yonemura:** Supervision. **Hiroyuki Harada:** Supervision. **Endar Hidayat:** Writing – review & editing, Writing – original draft, Supervision, Methodology, Data curation, Conceptualization. **Nur Maisarah Mohamad Sarbani:** Writing – review & editing, Writing – original draft, Validation. **Helmi Baharuddin Susanto:** Writing – original draft, Validation, Investigation, Formal analysis. **Yaressa Vaskah Situngkir:** Investigation, Formal analysis.

Data Availability

Data will be made available on request.

Declaration of Competing Interest

The authors declare that they have no known competing financial interests or personal relationships that could have appeared to influence the work reported in this paper.

Acknowledgement

E. H and NMMS express appreciation to the MEXT Scholarship for funding their studies at the Prefectural University of Hiroshima, Japan. E.H thank to National Institute for Materials Science (NIMS) for accepted internship program. Lastly, HBS, YVS, and MWC extend their gratitude to the Prefectural University of Hiroshima for accepted as exchange students.

References

[1] Liu J, Guo D, Zhou Y, Wu Z, Li W, Zhao F, Zheng X. Identification of ancient textiles from Yingpan, Xinjiang, by multiple analytical techniques. J Archaeol Sci 2011;38:1763–70. https://doi.org/10.1016/j.jas.2011.03.017.
[2] Al-Tohamy R, Ali SS, Li F, Okasha KM, Mahmoud YAG, Elsamahy T, Jiao H, Fu Y, Sun J. A critical review on the treatment of dye-containing wastewater: Ecotoxicological and health concerns of textile dyes and possible remediation approaches for environmental safety. Ecotoxicol Environ Saf 2022;231. https://doi.org/10.1016/j.ecoenv.2021.113160.
[3] RAI HS, BHATTACHARYYA MS, SINGH J, BANSAL TK, VATS P, BANERJEE UC. Removal of dyes from the effluent of textile and dyestuff manufacturing industry: a review of emerging techniques with reference to biological treatment. Crit Rev Environ Sci Technol 2005;35:219–38. https://doi.org/10.1080/10643380590917932.
[4] Liu J, Wang N, Zhang H, Baeyens J. Adsorption of Congo red dye on FexCo3-xO4 nanoparticles. J Environ Manag 2019;238:473–83. https://doi.org/10.1016/j.jenvman.2019.03.009.
[5] A. Gürses, M. Açıkyıldız, K. Güneş, M.S. Gürses, Classification of Dye and Pigments, in: 2016: pp. 31–45. 〈https://doi.org/10.1007/978–3-319–33892-7_3〉.
[6] Radoor S, Karayil J, Parameswaranpillai J, Siengchin S. Removal of anionic dye Congo red from aqueous environment using polyvinyl alcohol/sodium alginate/ZSM-5 zeolite membrane. Sci Rep 2020;10. https://doi.org/10.1038/s41598-020-72398-5.
[7] Khadhraoui M, Trabelsi H, Ksibi M, Bouguerra S, Elleuch B. Discoloration and detoxicification of a Congo red dye solution by means of ozone treatment for a possible water reuse. J Hazard Mater 2009;161:974–81. https://doi.org/10.1016/j.jhazmat.2008.04.060.
[8] Kristianto H, Rahman H, Prasetyo S, Sugih AK. Removal of Congo red aqueous solution using Leucaena leucocephala seed's extract as natural coagulant. Appl Water Sci 2019;9:88. https://doi.org/10.1007/s13201-019-0972-2.
[9] Khumalo NP, Vilakati GD, Mhlanga SD, Kuvarega AT, Mamba BB, Li J, Dlamini DS. Dual-functional ultrafiltration nano-enabled PSf/PVA membrane for the removal of Congo red dye. J Water Process Eng 2019;31:100878. https://doi.org/10.1016/j.jwpe.2019.100878.
[10] Akhtar A, Aslam Z, Asghar A, Bello MM, Raman AAA. Electrocoagulation of Congo red dye-containing wastewater: optimization of operational parameters and process mechanism. J Environ Chem Eng 2020;8:104055. https://doi.org/10.1016/j.jece.2020.104055.

[11] Sathishkumar K, AlSalhi MS, Sanganyado E, Devanesan S, Arulprakash A, Rajasekar A. Sequential electrochemical oxidation and bio-treatment of the azo dye congo red and textile effluent. J Photochem Photobio B 2019;200:111655. https://doi.org/10.1016/j.jphotobiol.2019.111655.
[12] Khan AA, Naqvi SR, Ali I, Farooq W, Anjum MW, AlMohamadi H, Lam SS, Verma M, Ng HS, Liew RK. Algal biochar: a natural solution for the removal of Congo red dye from textile wastewater. J Taiwan Inst Chem Eng 2023:105312. https://doi.org/10.1016/j.jtice.2023.105312.
[13] Khamparia S, Jaspal D. Technologies for Treatment of Colored Wastewater from Different Industries. Handbook of Environmental Materials Management. Cham: Springer International Publishing,; 2018. p. 1–14. https://doi.org/10.1007/978-3-319-58538-3_8-1.
[14] Rahmani M, Dadvand Koohi A. Adsorption of malachite green on the modified montmorillonite/xanthan gum-sodium alginate hybrid nanocomposite. Polym Bull 2022;79:8241–67. https://doi.org/10.1007/s00289-021-03889-2.
[15] Hidayat E, Harada H, Mitoma Y, Yonemura S, Halem HIA. Rapid removal of acid red 88 by zeolite/chitosan hydrogel in aqueous solution. Polymers 2022;14. https://doi.org/10.3390/polym14050893.
[16] Munagapati VS, Yarramuthi V, Kim Y, Lee KM, Kim DS. Removal of anionic dyes (Reactive Black 5 and Congo Red) from aqueous solutions using Banana Peel Powder as an adsorbent. Ecotoxicol Environ Saf 2018;148:601–7. https://doi.org/10.1016/j.ecoenv.2017.10.075.
[17] Aslam U, Javed T. Potential of Citrus limetta peel powder (CLPP) for adsorption of hazardous Congo red dye from wastewater. Water Pr Technol 2023;18:1051–73. https://doi.org/10.2166/wpt.2023.068.
[18] Li Y, Meas A, Shan S, Yang R, Gai X. Production and optimization of bamboo hydrochars for adsorption of Congo red and 2-naphthol. Bioresour Technol 2016;207:379–86. https://doi.org/10.1016/j.biortech.2016.02.012.
[19] Chawla S, Uppal H, Yadav M, Bahadur N, Singh N. Zinc peroxide nanomaterial as an adsorbent for removal of Congo red dye from waste water. Ecotoxicol Environ Saf 2017;135:68–74. https://doi.org/10.1016/j.ecoenv.2016.09.017.
[20] Zhao J, Lu Z, He X, Zhang X, Li Q, Xia T, Zhang W, Lu C. Fabrication and Characterization of Highly Porous Fe(OH)3@Cellulose Hybrid Fibers for Effective Removal of Congo Red from Contaminated Water. ACS Sustain Chem Eng 2017;5:7723–32. https://doi.org/10.1021/acssuschemeng.7b01175.
[21] Ahmad R, Kumar R. Adsorptive removal of congo red dye from aqueous solution using bael shell carbon. Appl Surf Sci 2010;257:1628–33. https://doi.org/10.1016/j.apsusc.2010.08.111.
[22] Baigorria E, Cano LA, Sanchez LM, Alvarez VA, Ollier RP. Bentonite-composite polyvinyl alcohol/alginate hydrogel beads: Preparation, characterization and their use as arsenic removal devices. Environ Nanotechnol Monit Manag 2020;14. https://doi.org/10.1016/j.enmm.2020.100364.
[23] Chen T, Liu H, Gao J, Hu G, Zhao Y, Tang X, Han X. Efficient removal of methylene blue by bio-based sodium alginate/lignin composite hydrogel beads. Polymers 2022;14. https://doi.org/10.3390/polym14142917.
[24] Frent OD, Vicas LG, Duteanu N, Morgovan CM, Jurca T, Pallag A, Muresan ME, Filip SM, Lucaciu RL, Marian E. Sodium Alginate—Natural Microencapsulation Material of Polymeric Microparticles. Int J Mol Sci 2022;23. https://doi.org/10.3390/ijms232012108.
[25] Tang S, Zhao Y, Wang H, Wang Y, Zhu H, Chen Y, Chen S, Jin S, Yang Z, Li P, Li S. Preparation of the sodium alginate-g-(polyacrylic acid-co-allyltrimethylammonium chloride) polyampholytic superabsorbent polymer and its dye adsorption property. Mar Drugs 2018;16. https://doi.org/10.3390/md16120476.
[26] Hidayat E, Sarbani NMM, Lahiri SK, Samitsu S, Yonemura S, Mitoma Y, Harada H. Effects of sodium alginate-poly(acrylic acid) cross-linked hydrogel beads on soil conditioner in the absence and presence of phosphate and carbonate ions. Case Stud Chem Environ Eng 2024;9:100642. https://doi.org/10.1016/j.cscee.2024.100642.
[27] Thakur S, Arotiba OA. Synthesis, swelling and adsorption studies of a pH-responsive sodium alginate–poly(acrylic acid) superabsorbent hydrogel. Polym Bull 2018;75:4587–606. https://doi.org/10.1007/s00289-018-2287-0.
[28] Merakchi A, Bettayeb S, Drouiche N, Adour L, Lounici H. Cross-linking and modification of sodium alginate biopolymer for dye removal in aqueous solution. Polym Bull 2019;76:3535–54. https://doi.org/10.1007/s00289-018-2557-x.
[29] Aljeboree AM, Alkaim AF. Studying removal of anionic dye by prepared highly adsorbent surface hydrogel nanocomposite as an applicable for aqueous solution. Sci Rep 2024;14:9102. https://doi.org/10.1038/s41598-024-59545-y.
[30] Mokeddem A, Benykhlef S, Bendaoudi AA, Boudouaia N, Mahmoudi H, Bengharez Z, Topel SD, Topel Ö. Sodium Alginate-based composite films for effective removal of congo red and coralene dark red 2b dyes: kinetic, isotherm and thermodynamic analysis. Water 2023;15:1709. https://doi.org/10.3390/w15091709.
[31] Lal Maurya K, Swain G, Kumar Sonwani R, Verma A, Sharan Singh R. Biodegradation of Congo red dye using polyurethane foam-based biocarrier combined with activated carbon and sodium alginate: batch and continuous study. Bioresour Technol 2022;351:126999. https://doi.org/10.1016/j.biortech.2022.126999.
[32] Hua Z, Pan Y, Hong Q. Adsorption of Congo red dye in water by orange peel biochar modified with CTAB. RSC Adv 2023;13:12502–8. https://doi.org/10.1039/D3RA01444D.
[33] Al- Rubai HF, Al-dahan AKH, Jasim BA. Green Synthesis of Iron Oxide Nanoparticles and Their Modification with CTAB for the Decolorization of Dye Reactive Blue 238. Iraqi J Sci 2023:1592–600. https://doi.org/10.24996/ijs.2023.64.4.2.
[34] Prajapati AK, Mondal MK. Novel green strategy for CuO–ZnO–C nanocomposites fabrication using marigold (Tagetes spp.) flower petals extract with and without CTAB treatment for adsorption of Cr(VI) and Congo red dye. J Environ Manag 2021;290:112615. https://doi.org/10.1016/j.jenvman.2021.112615.
[35] Khalfallah A. Structure and Applications of Surfactants. Surfactants - Fundamental Concepts and Emerging Perspectives. IntechOpen,; 2024. https://doi.org/10.5772/intechopen.111401.
[36] Akl MA, Mostafa AG, Abdelaal MY, Nour MAK. Surfactant supported chitosan for efficient removal of Cr(VI) and anionic food stuff dyes from aquatic solutions. Sci Rep 2023;13:15786. https://doi.org/10.1038/s41598-023-43034-9.
[37] Tadros T. Surfactants. Encyclopedia of Colloid and Interface Science. Berlin, Heidelberg: Springer Berlin Heidelberg,; 2013. p. 1242–90. https://doi.org/10.1007/978-3-642-20665-8_40.
[38] Palmer M, Hatley H. The role of surfactants in wastewater treatment: Impact, removal and future techniques: A critical review. Water Res 2018;147:60–72. https://doi.org/10.1016/j.watres.2018.09.039.
[39] Zhu L, Yang H, He Y. Sodium dodecyl sulfate assisted synthesis hydroxyapatite for effective adsorption of methylene blue. J Dispers Sci Technol 2023;44:1618–27. https://doi.org/10.1080/01932691.2022.2030237.
[40] Azizi A, Abouda L, Cherifi H, Krika A, Krika F. Enzymatic regeneration of modified cork with sodium dodecyl through the cationic dye removal from aqueous solution. Desalin Water Treat 2022;265:157–63. https://doi.org/10.5004/dwt.2022.28626.
[41] Sarabadan M, Bashiri H, Mousavi SM. Efficient removal of crystal violet from solution by montmorillonite modified with docosyl-trimethylammonium chloride and sodium dodecyl sulfate: modelling, kinetics and equilibrium studies. Clay Min 2022;57:7–20. https://doi.org/10.1180/clm.2022.15.
[42] Hong M, Wang Y, Wang R, Sun Y, Yang R, Qu L, Li Z. Poly(sodium styrene sulfonate) functionalized graphene as a highly efficient adsorbent for cationic dye removal with a green regeneration strategy. J Phys Chem Solids 2021;152:109973. https://doi.org/10.1016/j.jpcs.2021.109973.
[43] Ouasfi N, Sabbar E, Khamliche L. Intercalated double layer hydroxide with sodium lauryl sulfate for cationic dye adsorption from aqueous solution. Nanotechnol Environ Eng 2022;7:647–60. https://doi.org/10.1007/s41204-021-00188-z.
[44] Kaur N, Sharma S, Khosla E. Role of Surfactants Cetyl Pyridinium Chloride (CPC) and Cetyltrimethyl Ammonium Bromide (CTAB) in the Reverse Micellar Extraction of Ternary Mixture of Acid Dyes from Textile Effluent. Tenside Surfactants Deterg 2018;55:498–503. https://doi.org/10.3139/113.110589.
[45] Hosseinpour S, Götz V, Peukert W. Effect of Surfactants on the Molecular Structure of the Buried Oil/Water Interface. Angew Chem Int Ed 2021;60:25143–50. https://doi.org/10.1002/anie.202110091.
[46] del Caño R, Gisbert-González JM, González-Rodríguez J, Sánchez-Obrero G, Madueño R, Blázquez M, Pineda T. Effective replacement of cetyltrimethylammonium bromide (CTAB) by mercaptoalkanoic acids on gold nanorod (AuNR) surfaces in aqueous solutions. Nanoscale 2020;12:658–68. https://doi.org/10.1039/C9NR09137H.
[47] Hua Z, Pan Y, Hong Q. Adsorption of Congo red dye in water by orange peel biochar modified with CTAB. RSC Adv 2023;13:12502–8. https://doi.org/10.1039/D3RA01444D.
[48] Lu F, Ding G, Ma X, Huang B, You L. Chitosan-gelatin/cetyltrimethylammonium bromide magnetic polymer composites as reusable high performance adsorbent for AR 18 removal. J Mol Liq 2023;391:123303. https://doi.org/10.1016/j.molliq.2023.123303.
[49] Zhu Y, Cui Y, Peng Y, Dai R, Chen H, Wang Y. Preparation of CTAB intercalated bentonite for ultrafast adsorption of anionic dyes and mechanism study. Colloids Surf A Physicochem Eng Asp 2023;658:130705. https://doi.org/10.1016/j.colsurfa.2022.130705.
[50] Yang H, Tejado A, Alam N, Antal M, van de Ven TGM. Films Prepared from Electrosterically Stabilized Nanocrystalline Cellulose. Langmuir 2012;28:7834–42. https://doi.org/10.1021/la2049663.
[51] Hidayat E, Yoshino T, Yonemura S, Mitoma Y, Harada H. Synthesis, Adsorption Isotherm and Kinetic Study of Alkaline- Treated Zeolite/Chitosan/Fe3 + Composites for Nitrate Removal from Aqueous Solution—Anion and Dye Effects. Gels 2022;8. https://doi.org/10.3390/gels8120782.
[52] Modrzejewska Z. Sorption mechanism of copper in chitosan hydrogel. React Funct Polym 2013;73:719–29. https://doi.org/10.1016/j.reactfunctpolym.2013.02.014.
[53] Qurrat-Ul-Ain, Khatoon J, Shah MR, Malik MI, Khan IAT, Khurshid S, Naz R. Convenient pH-responsive removal of Acid Black 1 by green l-histidine/iron oxide magnetic nanoadsorbent from water: Performance and mechanistic studies. RSC Adv 2019;9:2978–96. https://doi.org/10.1039/c8ra09279f.
[54] Patel A, Soni S, Mittal J, Mittal A, Arora C. Sequestration of crystal violet from aqueous solution using ash of black turmeric rhizome. Desalin Water Treat 2021;220:342–52. https://doi.org/10.5004/dwt.2021.26911.
[55] Naushad M, Ahamad T, Al-Maswari BM, Abdullah Alqadami A, Alshehri SM. Nickel ferrite bearing nitrogen-doped mesoporous carbon as efficient adsorbent for the removal of highly toxic metal ion from aqueous medium. Chem Eng J 2017;330:1351–60. https://doi.org/10.1016/j.cej.2017.08.079.
[56] Shayesteh H, Rahbar-Kelishami A, Norouzbeigi R. Evaluation of natural and cationic surfactant modified pumice for congo red removal in batch mode: Kinetic, equilibrium, and thermodynamic studies. J Mol Liq 2016;221:1–11. https://doi.org/10.1016/j.molliq.2016.05.053.
[57] Foroughi-dahr M, Abolghasemi H, Esmaieli M, Nazari G, Rasem B. Experimental study on the adsorptive behavior of Congo red in cationic surfactant-modified tea waste. Process Saf Environ Prot 2015;95:226–36. https://doi.org/10.1016/j.psep.2015.03.005.
[58] Hidayat E, Mohamad Sarbani NMB, Yonemura S, Mitoma Y, Harada H. Application of Box–Behnken Design to Optimize Phosphate Adsorption Conditions from Water onto Novel Adsorbent CS-ZL/ZrO/Fe3O4: Characterization, Equilibrium, Isotherm, Kinetic, and Desorption Studies. Int J Mol Sci 2023;24. https://doi.org/10.3390/ijms24119754.
[59] Sami AJ, Butt YN, Nasar S. Elimination of a Carcinogenic Anionic Dye Congo Red from Water Using Hydrogels Based on Chitosan, Acrylamide and Graphene Oxide. J Bioprocess Biotech 2018;08. https://doi.org/10.4172/2155-9821.1000334.

[60] Harja M, Buema G, Bucur D. Recent advances in removal of Congo Red dye by adsorption using an industrial waste. Sci Rep 2022;12:6087. https://doi.org/10.1038/s41598-022-10093-3.
[61] Gao HJ, Wang SF, Fang LM, Sun GA, Chen XP, Tang SN, Yang H, Sun GZ, Li DF. Nanostructured spinel-type M(M = Mg, Co, Zn)Cr2O4 oxides: novel adsorbents for aqueous Congo red removal. Mater Today Chem 2021;22:100593. https://doi.org/10.1016/j.mtchem.2021.100593.
[62] Alharbi RA, Alminderej FM, Al-Harby NF, Elmehbad NY, Mohamed NA. Preparation and Characterization of a New Bis-Uracil Chitosan-Based Hydrogel as Efficient Adsorbent for Removal of Anionic Congo Red Dye. Polym (Basel) 2023;15:1529. https://doi.org/10.3390/polym15061529.
[63] Zhao D, Shen X. Preparation of Chitosan-Diatomite/Calcium Alginate Composite Hydrogel Beads for the Adsorption of Congo Red Dye. Water (Basel) 2023;15:2254. https://doi.org/10.3390/w15122254.
[64] Fadimatou NM, Fotsing PN, Mandjewil A, Siewe JM, Vieillard J, Dotto GL, Woumfo ED, Ngueagni PT. Cetyltrimethylammonium bromide (CTAB) functionalization of sodium silicate from rice husks ash for Naphthol Green B and Congo Red adsorption. Emergent Mater 2024. https://doi.org/10.1007/s42247-024-00655-8.